

# Multi-task Over-the-Air Federated Learning: A Non-Orthogonal Transmission Approach

Haoming Ma, Xiaojun Yuan, *Senior Member, IEEE*, Dian Fan, Zhi Ding, *Fellow, IEEE*, Xin Wang, *Senior Member, IEEE*

**Abstract**—In this letter, we propose a multi-task over-the-air federated learning (MOAFL) framework, where multiple learning tasks share edge devices for data collection and learning models under the coordination of a edge server (ES). Specially, the model updates for all the tasks are transmitted and superimposed concurrently over a non-orthogonal uplink channel via over-the-air computation, and the aggregation results of all the tasks are reconstructed at the ES through an extended version of the turbo compressed sensing algorithm. Both the convergence analysis and numerical results demonstrate that the MOAFL framework can significantly reduce the uplink bandwidth consumption of multiple tasks without causing substantial learning performance degradation.

**Index Terms**—Federated learning, multi-task learning, over-the-air computation, turbo compressed sensing.

## I. INTRODUCTION

WITH massive amount of data at wireless edge devices, federated learning (FL) has emerged as a popular framework for training machine learning models by accessing data in a distributive and confidential manner. The FL framework [1] requires uploading local model updates of edge devices to a specific edge server (ES) for model aggregation. Owing to the large number of devices as well as high dimension of model parameters, the bandwidth of uplink communication poses typically a major bottleneck of the FL framework.

Many methods have been developed to reduce the communication load in federated edge learning. For example, the authors in [2], [3] proposed to reduce uplink data rates by sparsifying and compressing the local model updates before transmission. In [4], [5], the authors proposed to quantize each element of local updates to a low-precision discrete value. In [6], [7], over-the-air computation was used to speed up local update aggregation by exploiting radio superposition over shared physical channels. However, existing works mostly focused on single-task FL, which involves a dedicated wireless channel for a single learning task.

In this letter, we propose a more general FL framework for multi-task over-the-air federated learning (MOAFL), where

H. Ma, X. Yuan and D. Fan are with the Center for Intelligent Networking and Communications, the University of Electronic Science and Technology of China, Chengdu, China (e-mail:haomingma1@outlook.com; xjyuan@uestc.edu.cn; df@std.uestc.edu.cn). Z. Ding is with the Department of Electrical and Computer Engineering, University of California at Davis, Davis, CA 95616 USA (e-mail:zding@ucdavis.edu). X. Wang is with the Key Laboratory for Information Science of Electromagnetic Waves (MoE), Department of Communication Science and Engineering, Fudan University, Shanghai 200433, China (e-mail:xwang11@fudan.edu.cn). The corresponding author is Xiaojun Yuan.

multiple learning tasks share edge devices for data collection and a single ES for parameter learning, and model aggregations at the ES are through over-the-air computation simultaneously for all the tasks. More specifically, at every edge device, the local model updates of all tasks are first sparsified and compressed individually by following the approach of [2], [3], prior to being transmitted and aggregated on uplink channel. Model aggregations of the individual tasks are reconstructed at each ES, based on an extended version of the turbo compressed sensing (Turbo-CS) algorithm [8]. The proposed non-orthogonal transmission of multi-task model updates reduces the required bandwidth of the uplink communication, by overcoming inter-task interference. Convergence analysis and experimental simulations establish that our proposed MOAFL framework is able to withstand the inter-task interference, and significantly reduce the bandwidth consumption without substantial learning performance degradation.

## II. SYSTEM MODEL

### A. Multi-task FL Framework

Let  $[i]$  represent a natural integer set  $\{1, \dots, i\}$ . We consider a multi-task FL framework, in which  $M$  wireless local devices carry out  $N$  learning tasks with the local data samples  $D_{nm}, n \in [N], m \in [M]$  under the help of a ES, as depicted in Fig. 1. Each task  $n$  on device  $m$  has access to a dataset  $D_{nm}$ .

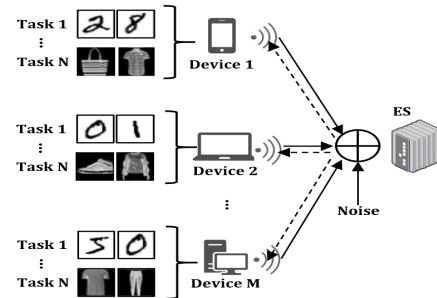


Fig. 1. An illustration of the multi-task FL framework.

The multi-task FL framework requires the minimization of the empirical loss function of each task  $n$  defined by

$$\mathcal{L}_n(\theta_n) = \sum_{m=1}^M K_{nm} \mathcal{L}_{nm}(\theta_n), \forall n \in [N] \quad (1)$$

with the local empirical loss function [9] of task  $n$  on device  $m$  decomposed into

$$\mathcal{L}_{nm}(\boldsymbol{\theta}_n) = \frac{1}{K_{nm}} \sum_{k=1}^{K_{nm}} l_n(\boldsymbol{\theta}_n; \mathbf{u}_{nmk}), \quad (2)$$

where  $l_n(\boldsymbol{\theta}_n; \mathbf{u}_{nmk})$  is the sample-wise loss function specified by task  $n$ ,  $\boldsymbol{\theta}_n \in \mathbb{R}^d$  denotes the model parameter of task  $n$  shared among the ES and participating terminals,  $\mathbf{u}_{nmk}$  denotes the  $k$ -th local data sample of  $D_{nm}$  of cardinality  $K_{nm} = |D_{nm}|$ .

The minimization of (1) is typically executed through distributed gradient descent. At the  $t$ -th communication round, the gradient  $\mathbf{g}_{nm}^{(t)} = \nabla \mathcal{L}_{nm}(\boldsymbol{\theta}_n) \in \mathbb{R}^d$  from each device  $m$  is sent to the ES over a wireless uplink with which the model parameter  $\boldsymbol{\theta}_n^{(t)}$  is updated via

$$\boldsymbol{\theta}_n^{(t+1)} = \boldsymbol{\theta}_n^{(t)} - \eta_n^{(t)} \frac{\sum_{m=1}^M K_{nm} \mathbf{g}_{nm}^{(t)}}{\sum_{m=1}^M K_{nm}}, \quad \forall n \in [N], \quad (3)$$

where  $\eta_n^{(t)}$  is the predetermined learning rate of task  $n$ . After that,  $\{\boldsymbol{\theta}_n^{(t+1)}\}_{n=1}^N$  are broadcast to all the devices by the ES over a wireless downlink to synchronize the FL model of each device. This process continues until the model update converges.

### B. Over-the-Air Channel Model

To make full use of channel bandwidth, we basically follow over-the-air computation in [10]. Specifically, at the  $t$ -th communication round, the wireless uplink channel with limited bandwidth  $s$  (with  $s \leq d$ ) is given by

$$\tilde{\mathbf{y}}^{(t)} = \sum_{m=1}^M \tilde{\mathbf{x}}_m^{(t)} + \tilde{\mathbf{n}}, \quad (4)$$

where  $\tilde{\mathbf{y}}^{(t)} \in \mathbb{R}^s$  is the channel output vector received by the ES,  $\tilde{\mathbf{n}} \in \mathbb{R}^s$  is an independent additive white Gaussian noise (AWGN) vector with each element independent and identically distributed (i.i.d.) as  $\mathcal{N}(0, \sigma_e^2)$ , and  $\tilde{\mathbf{x}}_m^{(t)} = \Phi_m(\mathbf{g}_{1m}^{(t)}, \dots, \mathbf{g}_{Nm}^{(t)}) \in \mathbb{R}^s$  is an encoding function of device  $m$ , mapping the local gradients  $\{\mathbf{g}_{nm}^{(t)}\}_{n=1}^N$  into the channel input vector  $\tilde{\mathbf{x}}_m^{(t)}$ , with the details specified later in Section III. Then, the objective of the ES is to recover an approximate estimate of  $\frac{\sum_{m=1}^M K_{nm} \mathbf{g}_{nm}^{(t)}}{\sum_{m=1}^M K_{nm}}$  from  $\tilde{\mathbf{y}}^{(t)}$  for each task  $n$ , and update the model parameter as in (3). For simplicity, following the convention [6], we assume that the downlink transmission is error-free. During the training process, the power consumption of device  $m$  at each round  $t$  is constrained by

$$\|\tilde{\mathbf{x}}_m^{(t)}\|^2 \leq P, \quad (5)$$

where  $P$  is the common power budget of each device and  $\|\cdot\|$  denotes the  $l_2$  norm.

## III. MULTI-TASK OVER-THE-AIR FEDERATED LEARNING (MOAFL) FRAMEWORK

### A. Transceiver Design of MOAFL

1) *Transmitter Design*: We process the local gradients of each task  $n$  on device  $m$  by essentially following the approach

in [6]. Specifically, at each round  $t$ ,  $\mathbf{g}_{nm}^{(t)}$  is firstly added by the error accumulation term  $\Delta_{nm}^{(t)} \in \mathbb{R}^d$  [5] as

$$\mathbf{g}_{nm}^{ac(t)} = \mathbf{g}_{nm}^{(t)} + \Delta_{nm}^{(t)}, \quad \forall m \in [M], \forall n \in [N], \quad (6)$$

where  $\Delta_{nm}^{(t)}$  is accumulated in the previous rounds with  $\Delta_{nm}^{(1)}$  initialized to  $\mathbf{0}$ . Then we set all the elements of  $\mathbf{g}_{nm}^{ac(t)} \in \mathbb{R}^d$  but the  $k_n$  elements with the greatest absolute values to zero, defined by

$$\mathbf{g}_{nm}^{sp(t)} = sp(\mathbf{g}_{nm}^{ac(t)}) \in \mathbb{R}^d, \quad \forall m \in [M], \forall n \in [N]. \quad (7)$$

$\Delta_{nm}^{(t)}$  is updated by

$$\Delta_{nm}^{(t+1)} = \mathbf{g}_{nm}^{ac(t)} - \mathbf{g}_{nm}^{sp(t)}, \quad \forall m \in [M], \forall n \in [N]. \quad (8)$$

Then  $\mathbf{g}_{nm}^{sp(t)}$  is compressed into a low-dimensional vector  $\mathbf{g}_{nm}^{cp(t)} \in \mathbb{R}^s$  through a compression matrix  $\mathbf{A}_n \in \mathbb{R}^{s \times d}$  as

$$\mathbf{g}_{nm}^{cp(t)} = \mathbf{A}_n \mathbf{g}_{nm}^{sp(t)}, \quad \forall m \in [M], \forall n \in [N]. \quad (9)$$

Following [8], we employ a partial discrete cosine transform (DCT) matrix  $\mathbf{A}_n = \mathbf{S}_n \mathbf{F}$  for each task  $n$ , where the selection matrix  $\mathbf{S}_n \in \mathbb{R}^{s \times d}$  consists of  $s$  randomly selected and reordered rows of the  $d \times d$  identity matrix  $\mathbf{I}_d$  and the  $(m, n)$ -th entry of the unitary DCT matrix  $\mathbf{F} \in \mathbb{R}^{d \times d}$  is given by  $\frac{1}{\sqrt{d}} e^{-2\pi j(m-1)(n-1)/d}$  with  $j = \sqrt{-1}$ .

We are now ready to describe the design of  $\Phi_m(\cdot)$ . As a distinct feature of the MOAFL framework, we propose a superposition based non-orthogonal transmission scheme to support the multiplexing of the  $N$  learning tasks. In specific, with (6)-(9), for each device  $m$ , we design

$$\tilde{\mathbf{x}}_m^{(t)} = \Phi_m(\mathbf{g}_{1m}^{(t)}, \dots, \mathbf{g}_{Nm}^{(t)}) = \sum_{n=1}^N \sqrt{\alpha_n^{(t)}} K_{nm} \mathbf{g}_{nm}^{cp(t)}, \quad (10)$$

where the coefficient  $\alpha_n^{(t)}$  is chosen to satisfy the constraint (5) and control the transmission power of each task  $n$ .

2) *Receiver Design*: We now describe the receiver design of the ES. We assume that the ES knows the power control coefficient  $\alpha_n^{(t)}$  and the size of dataset  $K_{nm}$  at each round  $t$ , and obtains  $\tilde{\mathbf{y}}^{(t)}$  over the wireless uplink in (4). With (9)-(10) and appropriate scaling, (4) is rewritten as

$$\mathbf{y}^{(t)} = [\mathbf{A}_1, \dots, \mathbf{A}_N] \left[ \mathbf{g}_1^{(t)T}, \dots, \mathbf{g}_N^{(t)T} \right]^T + \mathbf{n}, \quad (11)$$

where  $\mathbf{y}^{(t)} \triangleq \frac{\tilde{\mathbf{y}}^{(t)}}{\sqrt{\alpha_n^{(t)} \sum_{m=1}^M K_{nm}}}$ ,  $\mathbf{g}_n^{(t)} \triangleq \frac{\sum_{m=1}^M K_{nm} \mathbf{g}_{nm}^{sp(t)}}{\sum_{m=1}^M K_{nm}}$  is the sparsified version of  $\frac{\sum_{m=1}^M K_{nm} \mathbf{g}_{nm}^{(t)}}{\sum_{m=1}^M K_{nm}}$  in (3) and  $\mathbf{n} \triangleq \frac{\tilde{\mathbf{n}}}{\sqrt{\alpha_n^{(t)} \sum_{m=1}^M K_{nm}}}$  follows  $\mathcal{N}(0, \sigma^2)$  with  $\sigma \triangleq \frac{\sigma_e}{\sqrt{\alpha_n^{(t)} \sum_{m=1}^M K_{nm}}}$ . Then, given  $\mathbf{y}^{(t)}$ , the ES reconstructs each  $\mathbf{g}_n^{(t)}$  as  $\hat{\mathbf{g}}_n^{(t)}$ , which is subsequently used to update the model parameters via

$$\boldsymbol{\theta}_n^{(t+1)} = \boldsymbol{\theta}_n^{(t)} - \eta_n^{(t)} \hat{\mathbf{g}}_n^{(t)}, \quad \forall n \in [N], \quad (12)$$

where  $\eta_n^{(t)}$  is defined below (3).

The recovery of  $\{\mathbf{g}_n^{(t)}\}_{n=1}^N$  from  $\mathbf{y}^{(t)}$  in (11) is a compressive sensing (CS) problem with the compression matrix composed of  $N$  partial DCT matrices. Since the compression

matrix is partial orthogonal, we propose to employ the Turbo-CS algorithm developed in [8] to efficiently solve the CS problem. As each  $\mathbf{g}_n^{(t)}$  is the gradient for a different task  $n$ ,  $\{\mathbf{g}_n^{(t)}\}_{n=1}^N$  generally have different prior distributions. We assume that the entries of  $\mathbf{g}_n^{(t)}$  are independently drawn from a Bernoulli Gaussian distribution:

$$g_{n,k}^{(t)} \sim \begin{cases} 0 & \text{probability} = 1 - \lambda_n^{(t)}, \\ \mathcal{N}(0, v_n^{(t)}) & \text{probability} = \lambda_n^{(t)}, \end{cases} \quad (13)$$

where  $g_{n,k}^{(t)}$  is the  $k$ -th element of  $\mathbf{g}_n^{(t)}$ ,  $\lambda_n^{(t)}$  is the sparsity of  $\mathbf{g}_n^{(t)}$ , and  $v_n^{(t)}$  is the variance of the nonzero elements in  $\mathbf{g}_n^{(t)}$ . With the above prior model, we modify the Turbo-CS algorithm as follows.

As shown in Fig. 2, Turbo-CS iterates between two modules where module A handles the linear constraint in (11) and module B denoises the output from module A by exploiting the gradient sparsity in (13). Besides, the iterative process of Turbo-CS is carried out once at every round  $t$  and we drop out the round index  $t$  in the following for brevity.

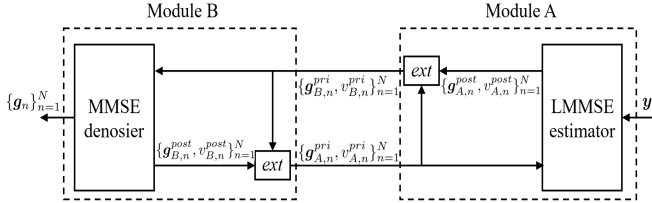


Fig. 2. An illustration of the Turbo-CS algorithm.

At each turbo iteration, given the prior mean  $\mathbf{g}_{A,n}^{pri} \in \mathbb{R}^d$  and the variance  $v_{A,n}^{pri} \in \mathbb{R}$  from module B as well as the observed vector  $\mathbf{y}$  in (11), the posterior mean  $\mathbf{g}_{A,n}^{post} \in \mathbb{R}^d$  and the variance  $v_{A,n}^{post} \in \mathbb{R}$  of  $\mathbf{g}_n$  are given by

$$\mathbf{g}_{A,n}^{post} = \mathbf{g}_{A,n}^{pri} + \frac{v_{A,n}^{pri} \mathbf{A}_n^T (\mathbf{y} - \sum_{k=1}^N \mathbf{A}_k \mathbf{g}_{A,k}^{pri})}{\sum_{k=1}^N v_{A,k}^{pri} + \sigma^2}, \forall n \in [N], \quad (14a)$$

$$v_{A,n}^{post} = v_{A,n}^{pri} - \frac{s}{d} \frac{v_{A,n}^{pri 2}}{\sum_{k=1}^N v_{A,k}^{pri} + \sigma^2}, \forall n \in [N]. \quad (14b)$$

From (14), the prior mean  $\mathbf{g}_{B,n}^{pri} \in \mathbb{R}^d$  and the variance  $v_{B,n}^{pri} \in \mathbb{R}$  of the MMSE denoiser are the extrinsic mean and variance from module A given by

$$\mathbf{g}_{B,n}^{pri} = v_{B,n}^{pri} \left( \frac{\mathbf{g}_{A,n}^{post}}{v_{A,n}^{post}} - \frac{\mathbf{g}_{A,n}^{pri}}{v_{A,n}^{pri}} \right), \forall n \in [N], \quad (15a)$$

$$v_{B,n}^{pri} = \left( \frac{1}{v_{A,n}^{post}} - \frac{1}{v_{A,n}^{pri}} \right)^{-1}, \forall n \in [N]. \quad (15b)$$

Then, each  $\mathbf{g}_{B,n}^{pri}$  is modeled as an observation of  $\mathbf{g}_n$  corrupted by additive noise  $\mathbf{n}_n$ :

$$\mathbf{g}_{B,n}^{pri} = \mathbf{g}_n + \mathbf{n}_n, \quad (16)$$

where  $\mathbf{n}_n \sim \mathcal{N}(0, v_{B,n}^{pri})$  is independent of  $\mathbf{g}_n$ . The posterior mean  $\mathbf{g}_{B,n}^{post} \in \mathbb{R}^d$  and the variance  $v_{B,n}^{post} \in \mathbb{R}$  of the MMSE denoiser are given by

$$\mathbf{g}_{B,n}^{post} = E[\mathbf{g}_n | \mathbf{g}_{B,n}^{pri}], \forall n \in [N], \quad (17a)$$

$$v_{B,n}^{post} = \sum_{k=1}^d \text{var}[g_{n,k} | g_{B,n,k}^{pri}], \forall n \in [N], \quad (17b)$$

where the expectation  $E$  is with respect to  $\mathbf{g}_n$ ,  $\text{var}[a|b] = E[(a - E[a|b])^2 | b]$  and  $g_{n,k}$  or  $g_{B,n,k}^{pri}$  is the  $k$ -th element of  $\mathbf{g}_n$  or  $\mathbf{g}_{B,n}^{pri}$ , respectively. The prior mean  $\mathbf{x}_{A,n}^{pri} \in \mathbb{R}^d$  and the variance  $v_{A,n}^{pri} \in \mathbb{R}$  of module A are updated by

$$\mathbf{g}_{A,n}^{pri} = v_{A,n}^{pri} \left( \frac{\mathbf{g}_{B,n}^{post}}{v_{B,n}^{post}} - \frac{\mathbf{g}_{B,n}^{pri}}{v_{B,n}^{pri}} \right), \forall n \in [N], \quad (18a)$$

$$v_{A,n}^{pri} = \left( \frac{1}{v_{B,n}^{post}} - \frac{1}{v_{B,n}^{pri}} \right)^{-1}, \forall n \in [N]. \quad (18b)$$

To sum up, given the initialization values  $\mathbf{g}_{A,n}^{pri} = \mathbf{0}$  and  $v_{A,n}^{pri} = v_n^{ini}$  for  $\forall n \in [N]$ , (14)-(18) iterate until some termination criterion is met, and  $\hat{\mathbf{g}}_n = \mathbf{g}_{B,n}^{post}$ ,  $\forall n \in [N]$  is for the model update in (12). Here,  $v_n^{ini}$  can be set to  $v_n$  in (13). But in practice,  $\{v_n\}_{n=1}^N$  may be difficult to determine in prior. Empirically, the algorithm is not very sensitive to the initial variances, and thus we approximately set  $v_1^{ini} = \dots = v_N^{ini} = \frac{\|\mathbf{y}\|^2}{Ns}$ . The above process is summarized in Algorithm 1.

---

#### Algorithm 1 MOAFL algorithm.

---

- 1: **Initialize**  $\Delta_{nm}^{(1)} = \mathbf{0}$
  - 2: **for**  $t = 1, 2, \dots$  **do**
  - 3:   **Devices do:**
  - 4:    **for**  $m = 1, \dots, M$  **in parallel do**
  - 5:      **for**  $n = 1, \dots, N$  **in parallel do**
  - 6:        Compute  $\mathbf{g}_{nm}^{(t)}$  with respect to  $D_{nm}$  and  $\theta_n^{(t)}$
  - 7:        Compute  $\mathbf{g}_{nm}^{cp(t)}$  via (6)-(7) and (9) with  $\mathbf{g}_{nm}^{(t)}$
  - 8:        Compute  $\Delta_{nm}^{(t+1)}$  via (8)
  - 9:      **end for**
  - 10:     Compute  $\{\tilde{\mathbf{x}}_m^{(t)}\}_{m=1}^M$  via (10)
  - 11:    **end for**
  - 12:    Send  $\{\tilde{\mathbf{x}}_m^{(t)}\}_{m=1}^M$  to the ES via (4)
  - 13:    **ES does:**
  - 14:    **Initialize**  $\mathbf{g}_{A,n}^{pri} = \mathbf{0}$ ,  $v_{A,n}^{pri} = v_n^{ini}$ ,  $\forall n \in [N]$
  - 15:    **repeat**
  - 16:      Update  $\mathbf{g}_{B,n}^{post}$ ,  $\forall n \in [N]$ , via (14)-(18)
  - 17:      **until** Convergence
  - 18:       $\hat{\mathbf{g}}_n^{(t)} = \mathbf{g}_{B,n}^{post}$ ,  $\forall n \in [N]$
  - 19:       $\theta_n^{(t+1)} = \theta_n^{(t)} - \eta_n^{(t)} \hat{\mathbf{g}}_n^{(t)}$ ,  $\forall n \in [N]$
  - 20:      Broadcast  $\{\theta_n^{(t+1)}\}_{n=1}^N$  to all the devices
  - 21:    **end for**
- 

#### B. Performance Analysis of Turbo-CS

Compared with the original Turbo-CS algorithm in [8], the main difference is that each subvector  $\mathbf{g}_n$  in (11) has its individual prior distribution in (13). Therefore, we track the state of each  $\mathbf{g}_n$  with an individual MSE. Similar to the derivation in [11], combining (14b), (15b), (17b) and (18b), the state evolution (SE) of Turbo-CS is given by

$$v_{B,n}^{pri} = \frac{d}{s} \left( \sum_{k=1}^N v_{A,k}^{pri} + \sigma^2 \right) - v_{A,n}^{pri}, \forall n \in [N], \quad (19a)$$

$$\frac{1}{v_{A,n}^{pri}} = \frac{1}{mmse_n(1/v_{B,n}^{pri})} - \frac{1}{v_{B,n}^{pri}}, \forall n \in [N], \quad (19b)$$

with  $mmse_n(1/v_{B,n}^{pri}) \equiv \mathbb{E}[\|\mathbf{g}_n - \mathbb{E}[\mathbf{g}_n | \mathbf{g}_n + \mathbf{n}_n]\|^2]$ . The fixed point of (19), denoted by  $\{v_n^*\}_{n=1}^N$ , tracks the normalized output MSEs of the Turbo-CS algorithm, where  $v_n^*$  is the MSE fixed point of  $\mathbf{g}_n$  for  $n = 1, \dots, N$ .

#### IV. CONVERGENCE ANALYSIS

Following the convention in stochastic optimization [12], we make some assumptions on the loss function  $\mathcal{L}_{nm}(\cdot)$  below:

*Assumption 1:*  $\mathcal{L}_{nm}(\cdot)$  is strongly convex with some (positive) parameter  $\omega$ . That is,  $\mathcal{L}_{nm}(\mathbf{y}) \geq \mathcal{L}_{nm}(\mathbf{x}) + (\mathbf{y} - \mathbf{x})^T \nabla \mathcal{L}_{nm}(\mathbf{x}) + \frac{\omega}{2} \|\mathbf{y} - \mathbf{x}\|^2, \forall \mathbf{x}, \mathbf{y} \in \mathbb{R}^d$ .

*Assumption 2:* The gradient  $\nabla \mathcal{L}_{nm}(\cdot)$  is Lipschitz continuous with some (positive) parameter  $L$ . That is,  $\|\nabla \mathcal{L}_{nm}(\mathbf{x}) - \nabla \mathcal{L}_{nm}(\mathbf{y})\| \leq L \|\mathbf{x} - \mathbf{y}\|, \forall \mathbf{x}, \mathbf{y} \in \mathbb{R}^d$ .

*Assumption 3:*  $\mathcal{L}_{nm}(\cdot)$  is twice-continuously differentiable.

*Assumption 4:* The gradient with respect to any training sample, denoted by  $\nabla l_n(\boldsymbol{\theta}_n; \cdot)$ , is upper bounded at  $\boldsymbol{\theta}_n$  as

$$\|\nabla l_n(\boldsymbol{\theta}_n, \mathbf{u}_{nmk})\|^2 \leq \alpha_1 + \alpha_2 \cdot \|\nabla \mathcal{L}_{nm}(\boldsymbol{\theta}_n)\|^2$$

for some constants  $\alpha_1 \geq 0$  and  $\alpha_2 > 0$ .

With (3) and (12), we analyze the model updating error vector  $\mathbf{e}_n^{(t)} \in \mathbb{R}^d$  at the  $t$ -th round caused by the sparsification step in (7) and the imperfect recovery of Turbo-CS as

$$\begin{aligned} \mathbf{e}_n^{(t)} &= \underbrace{\frac{\sum_{m=1}^M K_{nm}(\mathbf{g}_{nm}^{(t)} - \mathbf{g}_{nm}^{sp(t)})}{\sum_{m=1}^M K_{nm}}}_{\text{Sparsification error}} + \underbrace{\frac{\sum_{m=1}^M K_{nm} \mathbf{g}_{nm}^{sp(t)}}{\sum_{m=1}^M K_{nm}} - \hat{\mathbf{g}}_n^{(t)}}_{\text{Estimation error from Turbo-CS}} \\ &= \mathbf{e}_{1,n}^{(t)} + \mathbf{e}_{2,n}^{(t)}, \forall n \in [N], \end{aligned} \quad (20)$$

where  $\mathbf{e}_{1,n}^{(t)} \in \mathbb{R}^d$  and  $\mathbf{e}_{2,n}^{(t)} \in \mathbb{R}^d$  denote the sparsification error vector and the estimation error vector of Turbo-CS, respectively. Then we bound  $\|\mathbf{e}_{1,n}^{(t)}\|$  and  $\|\mathbf{e}_{2,n}^{(t)}\|$  in the following lemmas.

*Lemma 1:* Assume  $\|\mathbf{g}_{nm}^{(t)}\| \leq G$  for  $\forall n, m, t$ , where  $G$  is a constant. Then,  $\|\mathbf{e}_{1,n}^{(t)}\|$  is bounded as

$$\|\mathbf{e}_{1,n}^{(t)}\| \leq \frac{G(2r_n - r_n^t - r_n^{t+1})}{1 - r_n}, \forall n \in [N], \forall t = 1, 2, \dots, \quad (21)$$

where  $r_n = \sqrt{(d - k_n)/d} < 1$  with  $k_n$  defined above (7).

*Proof:* See Appendix A. ■

*Lemma 2:*  $\|\mathbf{e}_{2,n}^{(t)}\|$  is bounded as

$$\|\mathbf{e}_{2,n}^{(t)}\| = \sqrt{dv_n^*(t)} \leq \sqrt{dD}, \forall n \in [N], \forall t = 1, 2, \dots, \quad (22)$$

where  $v_n^*$  is the MSE fixed point on task  $n$  defined below (19b), and  $D$  is a certain constant.

*Proof:* Due to constraint (5), for  $\forall n \in [N]$ , the power of  $\mathbf{g}_n^{(t)}$  can be bounded by a constant, i.e.,  $v_n^{ini(t)} \leq D$ , where  $D$  is a constant. Besides, from the performance analysis of Turbo-CS in Section III-B, we know Turbo-CS converges to the fixed point  $\{v_n^*(t)\}_{n=1}^N$  at the  $t$ -th round with  $v_n^*(t) \leq v_n^{ini(t)}$ , for  $\forall n \in [N]$ . Thus,  $v_n^*(t) \leq D$ , which completes the proof. ■

We are now ready to present an upper bound on the loss  $\mathcal{L}_{nm}$  as follows.

*Theorem 1:* With Assumptions 1-4 and the assumption in Lemma 1, the MOAFL algorithm satisfies the weak convergence as

$$\mathcal{L}_{nm}(\boldsymbol{\theta}_n^{(t)}) - \mathcal{L}_{nm}(\boldsymbol{\theta}_n^*) \leq (1 - \omega/L)^t (\mathcal{L}_{nm}(\boldsymbol{\theta}_n^{(1)}) - \mathcal{L}_{nm}(\boldsymbol{\theta}_n^*)) + \mathcal{O}(C_n^{(t)}), \forall n \in [N], \quad (23)$$

where  $C_n^{(t)} = \max\{B_n^{(t)}, (1 - \omega/L + \epsilon)^t\}$  with  $B_n^{(t)} = \left(\frac{G(2r_n - r_n^t - r_n^{t+1})}{1 - r_n} + \sqrt{dD}\right)^2$ , for  $n = 1, \dots, N$ .

*Proof:* From (20), we bound  $\|\mathbf{e}_n^{(t)}\|^2$  for  $\forall n \in [N]$  as

$$\|\mathbf{e}_n^{(t)}\|^2 \leq (\|\mathbf{e}_{n,1}^{(t)}\| + \|\mathbf{e}_{n,2}^{(t)}\|)^2 \leq B_n^{(t)}, \quad (24)$$

with  $B_n^{(t)} = \left(\frac{G(2r_n - r_n^t - r_n^{t+1})}{1 - r_n} + \sqrt{dD}\right)^2$ , where the last step of (24) follows from Lemmas 1 and 2. Clearly,  $\lim_{t \rightarrow \infty} B_n^{(t+1)}/B_n^{(t)} \leq 1$ . Thus, based on Assumptions 1-4 and [12, Theorem 2.2], the MOAFL algorithm satisfies the weak convergence specified by (23). ■

#### V. EXPERIMENTAL RESULTS

In this section, we validate our system design with experiments. Specifically, we consider  $N = 2$  federated image classification tasks on the MNIST and the Fashion-MNIST datasets, respectively, among  $M = 20$  local devices and a ES. For each task, we train a convolutional neural network with  $d = 10920$  parameters utilizing gradient descent optimizer, two convolution layers and two fully connected layers.

In Fig. 3, the performance of each task is measured by test accuracy versus communication round  $t$ . For the single-task baseline, DSGD-FL [6] is applied with no interference from the other task. We observe that the test accuracy of MOAFL is comparable to that of the single-task scheme, and both schemes converge to an accuracy of 0.9 on the MNIST task as well as to an accuracy of 0.72 on the Fashion-MNIST task. Besides, the test accuracy of MOAFL is only about 2% lower than that of the ideal error-free scheme, which demonstrates the excellent interference suppression capability of MOAFL.

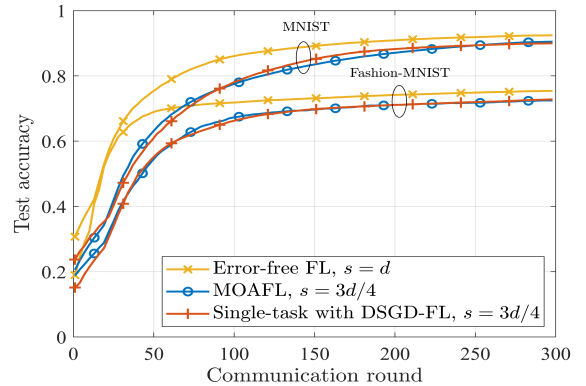


Fig. 3. Test accuracy on two tasks with  $M = 20, P = 0.25, k_1 = k_2 = 0.1d, \alpha_1^{(t)} = \alpha_2^{(t)} = 100t, \sigma_e^2 = 1, \eta_1^{(t)} = \eta_2^{(t)} = \frac{1}{10+t}, K_{nm} = 2500, \forall n \in [N], \forall m \in [M]$ .

For further comparison, we define  $\xi_n^{max}$  as the maximum test accuracy of each task  $n$ , and define  $t^*(\xi)$  as the total

required rounds of communications for every task  $n$  to reach its target accuracy  $\xi \cdot \xi_n^{max}$ , where  $\xi$  is called relative target accuracy. Thus,  $t^*(\xi)$  of MOAFL is given by

$$t^*(\xi) = \max\{t_1^*(\xi), \dots, t_N^*(\xi)\}. \quad (25)$$

where  $t_n^*(\xi)$  is the required communication rounds of task  $n$  to reach its target accuracy  $\xi \cdot \xi_n^{max}$ . We use a time division multiplexing (TDM) scheme, where each task is learned in an orthogonal time slot and DSGD-FL is applied in learning. Clearly,  $t^*(\xi)$  of TDM is given by

$$t^*(\xi) = \sum_{n=0}^N t_n^*(\xi). \quad (26)$$

Fig. 4 depicts the total required communication rounds  $t^*$  versus relative target accuracy  $\xi$ . We see that the total required communication rounds of MOAFL to complete the two tasks is about half of that of the TDM scheme at almost any value of  $\xi$ , which again demonstrates the superior performance of MOAFL.

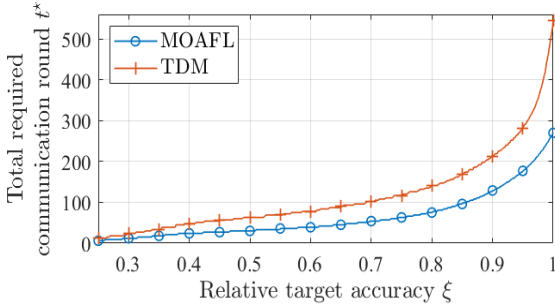


Fig. 4. The required communication rounds  $t^*$  of interference-free with TDM and MOAFL, with  $M = 20, P = 0.25, k_1 = k_2 = 0.1d, s = 3d/4, \xi_1^{max} = 0.90, \xi_2^{max} = 0.72, \alpha_1^{(t)} = \alpha_2^{(t)} = 100t, \sigma_e^2 = 1, \eta_1^{(t)} = \eta_2^{(t)} = \frac{1}{10+t}, K_{nm} = 2500, \forall n \in [N], \forall m \in [M]$ .

## VI. CONCLUSION

We developed a MOAFL framework with classic over-the-air computation to support multiple learning tasks over a non-orthogonal uplink channel. Furthermore, we modified the original Turbo-CS algorithm in the compressed sensing context to reconstruct the sparsified model aggregation updates at ES. Both the convergence analysis and experimental results showed that our proposed MOAFL framework is not sensitive to the inter-task interference, thereby leading to significant reduction in total bandwidth consumption with only slight learning performance degradation.

### APPENDIX A PROOF OF LEMMA 1

From (20), we bound  $\|e_{1,n}^{(t)}\|$  for  $\forall n$  at each round  $t$  as

$$\begin{aligned} \|e_{1,n}^{(t)}\| &= \left\| \frac{\sum_{m=1}^M K_{nm}(\mathbf{g}_{nm}^{(t)} - \mathbf{g}_{nm}^{sp(t)})}{\sum_{m=1}^M K_{nm}} \right\| \\ &\leq \frac{\sum_{m=1}^M K_{nm} \|\mathbf{g}_{nm}^{ac(t)} - \mathbf{g}_{nm}^{sp(t)} - \Delta_{nm}^{(t)}\|}{\sum_{m=1}^M K_{nm}} \end{aligned} \quad (27)$$

$$\leq \frac{\sum_{m=1}^M K_{nm} (\|\Delta_{nm}^{(t)}\| + \|\mathbf{g}_{nm}^{ac(t)} - \mathbf{g}_{nm}^{sp(t)}\|)}{\sum_{m=1}^M K_{nm}},$$

where the second step comes from (6) and the last step is from the triangular inequality. From (7),

$$\|\mathbf{g}_{nm}^{ac(t)} - \mathbf{g}_{nm}^{sp(t)}\| \leq r_n \|\mathbf{g}_{nm}^{ac(t)}\|, \quad (28)$$

where  $r_n = \sqrt{(d - k_n)/d}$ . Therefore,  $\|e_{1,n}^{(t)}\|$  is bounded as

$$\begin{aligned} \|e_{1,n}^{(t)}\| &\leq \frac{\sum_{m=1}^M K_{nm} (\|\Delta_{nm}^{(t)}\| + r_n \|\mathbf{g}_{nm}^{ac(t)}\|)}{\sum_{m=1}^M K_{nm}} \\ &\leq \frac{\sum_{m=1}^M K_{nm} ((1 + r_n) \|\Delta_{nm}^{(t)}\| + r_n \|\mathbf{g}_{nm}^{(t)}\|)}{\sum_{m=1}^M K_{nm}}, \end{aligned} \quad (29)$$

where the last inequality comes from (6) and the triangular inequality. Then,

$$\begin{aligned} \|\Delta_{nm}^{(t)}\| &= \|\mathbf{g}_{nm}^{ac(t-1)} - \mathbf{g}_{nm}^{sp(t-1)}\| \\ &\leq r_n \|\mathbf{g}_{nm}^{ac(t-1)}\| \\ &= r_n \|\mathbf{g}_{nm}^{(t-1)} + \Delta_{nm}^{(t-1)}\| \\ &\leq r_n (\|\mathbf{g}_{nm}^{(t-1)}\| + \|\Delta_{nm}^{(t-1)}\|), \end{aligned} \quad (30)$$

where the first step is from (8), and the second step is from (28). From (30), we obtain

$$\|\Delta_{nm}^{(t)}\| \leq \sum_{i=1}^{t-1} r_n^i \|\mathbf{g}_{nm}^{(t-i)}\|. \quad (31)$$

Finally, from the assumption in Lemma 1, combining (29) and (31), we obtain (21), which completes the proof.

## REFERENCES

- [1] J. Konečný, H. B. McMahan, D. Ramage, and P. Richtárik, "Federated optimization: Distributed machine learning for on-device intelligence," *arXiv:1610.02527*, Oct. 2016.
- [2] F. Sattler, S. Wiedemann, K.-R. Müller, and W. Samek, "Sparse binary compression: Towards distributed deep learning with minimal communication," *arXiv:1805.08768*, May 2018.
- [3] Y. Lin, S. Han, H. Mao, Y. Wang, and W. J. Dally, "Deep gradient compression: Reducing the communication bandwidth for distributed training," *arXiv:1712.01887*, Jun. 2020.
- [4] D. Alistarh, D. Grubic, J. Li, R. Tomioka, and M. Vojnovic, "QSGD: Communication-efficient SGD via gradient quantization and encoding," *arXiv:1610.02132*, Dec. 2017.
- [5] F. Seide, H. Fu, J. Droppo, G. Li, and D. Yu, "1-bit stochastic gradient descent and its application to data-parallel distributed training of speech DNNs," *Proc. INTERSPEECH*, 2014, pp. 1058–1062.
- [6] M. M. Amiri and D. Gündüz, "Machine learning at the wireless edge: Distributed stochastic gradient descent over-the-air," *IEEE Trans. Signal Process.*, vol. 68, pp. 2155–2169, 2020.
- [7] H. Liu, X. Yuan, and Y.-J. A. Zhang, "Reconfigurable intelligent surface enabled federated learning: A unified communication-learning design approach," *IEEE Trans. Wirel. Commun.*, pp. 1–1, 2021.
- [8] J. Ma, X. Yuan, and L. Ping, "Turbo compressed sensing with partial DFT sensing matrix," *IEEE Signal Process. Lett.*, vol. 22, no. 2, pp. 158–161, 2014.
- [9] Y. Zhang and L. Xiao, "Communication-efficient distributed optimization of self-concordant empirical loss," *arXiv:1501.00263*, Jan. 2015.
- [10] B. Nazer and M. Gastpar, "Computation over multiple-access channels," *IEEE Trans. Inf. Theory*, vol. 53, pp. 3498–3516, Nov. 2007.
- [11] J. Ma, X. Yuan, and L. Ping, "On the performance of turbo signal recovery with partial DFT sensing matrices," *IEEE Signal Process. Lett.*, pp. 1–1, 2015.
- [12] M. Friedlander and M. Schmidt, "Erratum: Hybrid deterministic-stochastic methods for data fitting," *Computing Research Repository - CORR*, vol. 34, Apr. 2011.